Evaluation of the mathematical Simpson's method for asbestos-cement detection in hyperspectral images

Evaluación del método matemático de Simpson en la detección de asbesto-cemento en imágenes hiperespectrales

Gabriel Elías Chanchí Golondrino[1]
Manuel Alejandro Ospina Alarcón[2]
Manuel Saba[3]

[1]PhD, Profesor de la Universidad de Cartagena, Universidad de Cartagena, Grupo de Investigación DaToS, Cartagena de Indias-Colombia
[2]PhD, Profesor de la Universidad de Cartagena, Universidad de Cartagena, Grupo de Investigación DaToS, Cartagena de Indias-Colombia
[3]PhD, Profesor de la Universidad de Cartagena, Universidad de Cartagena, Grupo de Investigación ESCONPAT, Cartagena de Indias-Colombia
gchanchig@unicartagena.edu.co

Cite this article as: G. Chanchí-Golondrino, M. Ospina-Alarcón, M. Saba "Evaluation of the mathematical Simpson's method for asbestos-cement detection in hyperspectral images", Prospectiva, Vol 23, N° 2, 2025.

Recibido: 19/01/2025 / Aceptado: 25/04/2025
http://doi.org/ 10.15665/rp.v23i2.3722

RESUMEN

A partir del desafío existente en las imágenes hiperespectrales relacionado con la identificación de métodos eficaces y eficientes en la detección de materiales, ante la alta dimensionalidad asociada a las bandas espectrales, en este artículo se propone como aporte un nuevo método para la detección de asbesto en imágenes hiperespectrales, basado en la aplicación del método de Simpson para el cálculo del área bajo la curva de la firma espectral del asbesto-cemento y la diferencia entre áreas con pixeles de asbesto y de otros materiales. Para el desarrollo de la presente investigación, fueron definidas 5 fases metodológicas a saber: F1. Obtención de los pixeles de muestra de asbesto-cemento y de otros materiales, F2. Determinación del píxel característico normalizado de asbesto-cemento y su área bajo la curva, F3. Implementación del método e identificación de los umbrales de detección con pixeles de asbesto y de otros materiales. F4. Despliegue del método sobre la imagen hiperespectral de referencia, F5. Evaluación de la eficacia y la eficiencia del método con respecto al método de la correlación. A nivel de los resultados, se obtuvo que el método propuesto obtuvo una mayor efectividad para la detección de asbesto-cemento entre las bandas 48 y 157. Del mismo modo, se obtuvo que a nivel computacional, el método propuesto es 1.79% más eficiente que el método de la correlación, el cual es uno de los más difundidos en la detección de materiales en imágenes hiperespectrales. A partir de los resultados obtenidos, el método propuesto puede servir de referencia para ser extrapolado en la detección de otros materiales en estas imágenes, así como ser integrado en sistemas de monitorización de materiales a partir de imágenes hiperespectrales.

Palabras clave: Imágenes hiperespectrales, detección de asbesto, método de Simpson, sensado remoto.

ABSTRACT

Based on the challenge in hyperspectral images related to identifying effective and efficient methods for material detection, given the high dimensionality associated with spectral bands, this article proposes a novel method for asbestos detection in hyperspectral images. The method is based on the application of Simpson's method to calculate the area under the curve of the asbestos-cement spectral signature and the difference between areas corresponding to pixels of asbestos and other materials. For the development of this research, five methodological phases were defined as follows: F1. Acquisition of sample pixels of asbestos-cement and other materials, F2. Determination of the normalized characteristic pixel of asbestos-cement and its area under the curve, F3. Implementation of the method and identification of detection thresholds using pixels of asbestos and other materials, F4. Deployment of the method on the reference hyperspectral image, F5. Evaluation of the method's effectiveness and efficiency compared to the correlation method. In terms of results, the proposed method showed greater effectiveness in detecting asbestos-cement within the spectral bands 48 to 157. Similarly, it was found that, computationally, the proposed method is 1.79% more efficient than the correlation method, which is one of the most widely used approaches for material detection in hyperspectral images. Based on these results, the proposed method can serve as a reference for extrapolation to the detection of other materials in these images and can also be integrated into material monitoring systems using hyperspectral images.

Keywords: Hyperspectral images, asbestos detection, Simpson's method, remote sensing.

1. Introduction

Remote sensing can be defined as a technology that enables the acquisition and processing of information about the characteristics of objects or areas on the Earth's surface without direct contact, using electromagnetic radiation as the means of interaction and sensors mounted on satellites, airplanes, or drones [1], [2], [3]. Among the main advantages of remote sensing is its ability to provide large-scale and real-time data efficiently, allowing the monitoring of environmental changes such as crop health or deforestation with a frequency that would be difficult to achieve through traditional methods, which are more limited in spatial and temporal scope [4], [5], [6], [7]. Furthermore, since remote sensing techniques are non-invasive, they do not alter the observed environment, unlike some traditional methods, which can be destructive or intrusive [8].

One of the most widely used remote sensing techniques is hyperspectral imaging, an advanced technology that combines spectroscopy with traditional imaging, enabling data capture in three dimensions: two spatial dimensions (x, y) and one spectral dimension (λ). This three-dimensional structure is known as a data cube due to its ability to store detailed information about the spectral composition of each pixel in an image [9], [10], [11]. In this structure, each layer of the data cube represents an image at a specific wavelength, allowing for the analysis of spectral variation across spatial dimensions [12]. In a hyperspectral image, each pixel corresponds to a vector containing information from multiple spectral bands, known as a spectral signature, which provides a detailed representation of the spectral properties of each material [13], [14]. Spectral signatures enable the accurate classification of different types of land cover, such as vegetation, rocks, artificial formations, and other materials, through the analysis of the unique spectral patterns of each material [15].

Several studies have been conducted on asbestos detection using hyperspectral images. For instance, in [16] and [17], hyperspectral images in the shortwave infrared range (SWIR: 1000–2500 nm) were used to detect asbestos minerals such as amosite, crocidolite, and chrysotile in cement matrices, employing principal component analysis (PCA) and soft independent modeling of class analogy (SIMCA) for sample classification. Similarly, in [18] and [19], hyperspectral images were used to identify and separate materials containing asbestos in construction and demolition waste, utilizing multivariate analysis methods for material classification. Finally, in [20] and [21], procedures have been developed for recognizing asbestos-cement roofs to assess their deterioration using hyperspectral images, enabling the mapping of asbestos-cement roofs and the estimation of asbestos fiber abundance on the surface.

In terms of the challenges in the field of hyperspectral imaging, it is important to note that these images contain a large number of spectral bands, resulting in high dimensionality. This increases computational costs and makes them difficult to process and analyze using traditional machine learning methods [22], [23], [24], [25]. Similarly, regarding the application of deep network-based models in the domain of hyperspectral images, the available training samples are often limited, making training challenging as it typically requires a large number of samples [25]. Moreover, the implementation of sophisticated techniques such as deep learning requires significant hardware and computational capacity to effectively address the detection and classification of materials [26]. Therefore, there is a need for alternative methods that are less complex and enable the effective and efficient detection of materials.

Based on the above, this article proposes a new method for detecting asbestos in hyperspectral images, which is based on comparing the areas under the curve of the characteristic pixel of asbestos with respect to the other pixels in the image, using Simpson's method for this purpose. This method for calculating the area divides the curve into an even number of equal subintervals, approximating each pair of subintervals with a parabola that passes through three equidistant points on the axis, allowing for a more accurate estimation by considering the curvature of the function [27], [28]. Compared to the trapezoidal rule, Simpson's method provides a better approximation of the area under the curve, especially when the curve is continuous and well-defined by the data points [29], [30]. The proposed method was implemented using open-source libraries such as spectral, scipy, numpy, pandas, and matplotlib, utilizing the implementation of Simpson's method provided by the scipy library through the simpson(y, x) function.

In this context, the proposed method offers a computationally efficient, low-cost, and easy-to-implement solution that does not require extensive training or large datasets. Unlike complex deep learning models that demand significant computational resources, this strategy provides a lightweight and effective alternative, making it suitable for deployment in resource-limited environments. This feature is particularly relevant for implementation in public health and environmental monitoring programs, where speed, simplicity, and reproducibility are essential.

It is worth mentioning that, initially, the proposed method was evaluated using a sample of asbestos-cement pixels and pixels from other materials, which were extracted from a reference hyperspectral image of the Manga neighborhood in the city of Cartagena. This evaluation allowed for the determination of the asbestos detection thresholds of the proposed method. Using these detection thresholds, the method was deployed on the full hyperspectral image, and its effectiveness in detecting asbestos was compared to the correlation method, which is one of the most widely used approaches for material detection in hyperspectral images [31]. Similarly, the computational efficiency of the method was evaluated in comparison to the correlation method by executing multiple repetitions of the method on a specific region of the reference image. The proposed method aims to serve as an alternative for integration into systems for monitoring and detecting materials using hyperspectral images. Furthermore, the proposed method is highly relevant to public health due to the implications of asbestos in the development of respiratory diseases among individuals exposed to this material [32], [33], [34].

In addition to its technical contribution, the proposed method has significant implications for public health, as it enables non-invasive identification of roofs containing asbestos-cement. Since prolonged exposure to asbestos is linked to serious diseases such as asbestosis, mesothelioma, and lung cancer, the early and accurate detection of this material through hyperspectral imaging can support preventive intervention programs, environmental monitoring, and remediation efforts in urban, rural, and industrial areas. This capability represents a major advancement for risk management systems in public health, especially in contexts where manual mapping is limited or unfeasible.

In contrast to widely used correlation methods, which rely on linear similarity measures and can be sensitive to spectral noise, the proposed method introduces a numerical integration approach that considers the full shape of the spectral curve, thereby improving material discrimination. Unlike deep learning approaches that require large volumes of labeled data and significant computational resources, the present method stands out for its low computational cost, ease of implementation, and adaptability to

various contexts. This combination of features represents a methodological innovation that has not been previously explored in asbestos-cement detection using hyperspectral images.

The remainder of the article is organized as follows: Section 2 presents the methodological phases considered for the development of this research. Section 3 describes the results obtained in this study, which include, first, the evaluation of the method using a set of sample pixels of asbestos-cement and other materials to identify the detection thresholds. Additionally, this section details the deployment of the method on the full reference image to determine the percentage of asbestos detected using the method and to compare the results with those obtained through the correlation method. Similarly, the computational efficiency of the method is evaluated in comparison to the correlation method by analyzing the average processing time obtained in 200 executions of both methods on a specific region of the reference hyperspectral image. Finally, Section 4 presents the conclusions and future work derived from this research.

2. Methodology

For the development of this research, five methodological phases were defined (see Figure 1): P1. Acquisition of sample pixels of asbestos-cement and other materials, P2. Determination of the normalized characteristic pixel of asbestos-cement and its area under the curve, P3. Implementation of the method and identification of detection thresholds using pixels of asbestos and other materials, P4. Deployment of the method on the reference hyperspectral image, and P5. Evaluation of the method's effectiveness and efficiency compared to the correlation method.

Figure 1. Methodology considered. Source: Own.

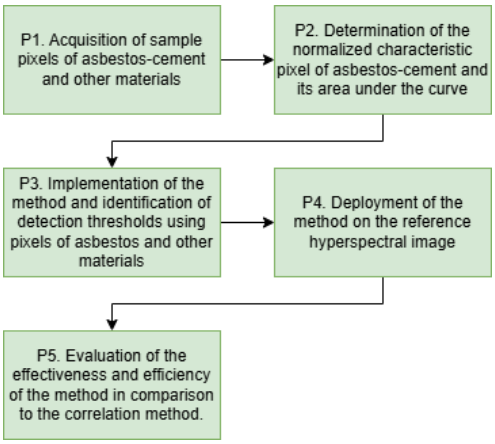

In Phase 1 of the methodology, a total of 75 sample pixels of asbestos-cement and 75 pixels of other materials (such as vegetation, water, roads, among others) were selected from a reference hyperspectral image corresponding to the Manga neighborhood in the city of Cartagena. This image consists of 725x850 pixels, each containing 380 reflectance bands. These sample pixels were obtained through visual inspection and are shown in Figure 2, which presents an RGB representation of the hyperspectral image, with asbestos pixels marked in blue and pixels of other materials marked in red. It is worth noting that these pixels will be used for training and evaluating the method, focusing on assessing the proposed method’s ability to differentiate asbestos-cement pixels.

Figure 2. Sample pixels of asbestos and other materials. Source: Own.

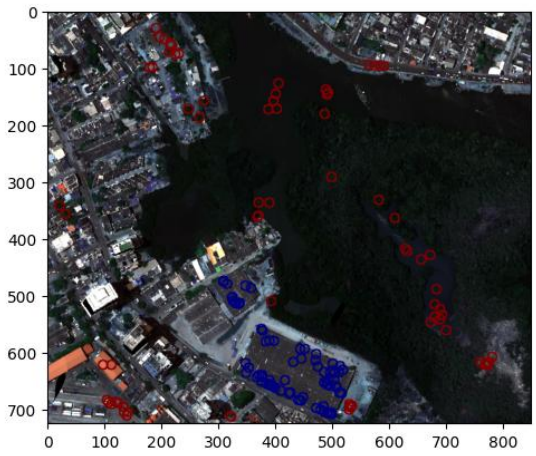

In Phase 2, using the 75 selected asbestos-cement pixels, each with a depth of 380 bands, the characteristic pixel of asbestos-cement was obtained. This pixel was calculated by taking the median of each reflectance band, leveraging the statistical operations provided by the NumPy and pandas libraries. Accordingly, Figure 3 shows the sample asbestos-cement pixels and the characteristic pixel obtained by calculating the median for each of the 380 bands.

Figure 3. Determination of the characteristic pixel of asbestos-cement. Source: Own.

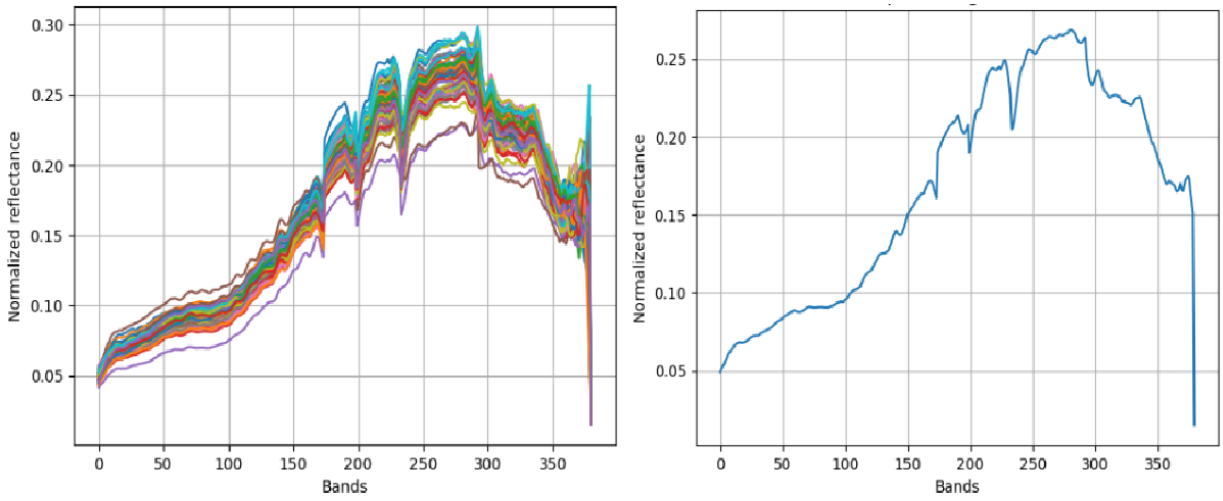

Similarly, based on the characteristic pixel, the area under the curve of the characteristic spectral signature was calculated using Simpson's method. This was implemented through the Simpson (y, x) function provided by the SciPy library in Python. This spectral signature area was later used in subsequent phases to compare it with the areas of other pixels in the image and to identify the similarity between the curves. Simpson's method is a numerical integration technique used to determine the area under the curve of a continuous or discretized function. This approach is particularly advantageous in applications involving spectral data, as it delivers precise results even with a limited number of sampling points [35]. The general formula of Simpson's method for calculating the definite integral of a function over an interval is [36]:

$$\int_a^b f(x)\,dx \approx \frac{h}{3}\left[f(x_0) + 4\sum_{i=1,3,5,\ldots}^{n-1} f(x_i) + 2\sum_{i=2,4,6,\ldots}^{n-2} f(x_i) + f(x_n)\right] \quad (2)$$

$$h = \frac{b-a}{n} \quad (3)$$

$$x_i = a + i \cdot h \quad para\ i=0,1,2,\ldots,n \ (4)$$

In Equation (2), *a* and *b* represent the lower and upper limits of integration, respectively. *n* is the number of subintervals, which must be even to apply this method [2]. *h* is the length of each subinterval and is calculated using Equation (3). The sampling points $x_0, x_1, \ldots, x_n$ are uniformly distributed within the interval [a, b] (dividing the interval into *n* equal parts) and are calculated using Equation (4). $f(x_0)$ and $f(x_n)$ are the function values at the endpoints of the interval. The summation $\sum_{i=1,3,5,\ldots}^{n-1} f(x_i)$ represents the terms weighted by 4, corresponding to the odd-indexed points, while $\sum_{i=2,4,6,\ldots}^{n-2} f(x_i)$ represents the terms weighted by 2, corresponding to the intermediate even-indexed points. In this manner, by utilizing Equations (2), (3), and (4) in hyperspectral images [37], the integration interval [a,b] represents the spectral range over which the analysis is conducted. In the context of hyperspectral images, this interval corresponds to the selected wavelengths [37]; n defines the total number of spectral sampling points. An even number ensures the correct application of the method. h is the spectral step, indicating the resolution between two consecutive bands in the spectral data. $f(x_i)$ represents the spectral intensities or reflectance response at each wavelength x_i [36], and the weights (1, 4, 2) are weighting factors that assign greater importance to the intermediate (odd-indexed) points and lesser importance to the even-indexed intermediate points. This Simpson's method has been widely used in spectral data analysis due to its superior accuracy compared to other numerical methods, with errors on the order of 10^{-3} for smooth functions and uniformly sampled spectral data [36]. Additionally, its computational efficiency reduces the number of operations required for integration in large datasets. In the context of hyperspectral images, the integration of the spectral curve for each pixel enables precise comparison of spectral signatures, allowing for the detection of specific materials such as asbestos-cement roofing [38].
In this context, during Phase 3 of the methodology, the proposed method was implemented and evaluated using the sample pixels of asbestos and other materials. For each pixel, the absolute value of the difference between areas was calculated, and the minimum and maximum differences with asbestos pixels and other material pixels were determined. The goal was to identify whether there was overlap between the maximum difference identified with asbestos pixels and the minimum difference with pixels of other materials. If overlap was found, band ranges without overlap were selected to identify the minimum and maximum detection thresholds for the method.

In Phase 4 of the methodology, once the thresholds and the bands without overlap were identified, the implemented method was applied to all the pixels in the reference image to determine the percentage of asbestos pixels relative to the total image. To achieve this, a pixel-by-pixel iteration was performed, calculating the area under the curve for each pixel and obtaining the absolute value of the difference. Based on the thresholds identified in the previous phase, each pixel was classified as either asbestos or another material. If the pixel was classified as asbestos, it was marked in blue on a copy of the reference image.

Finally, in Phase 5 of the methodology, the correlation method was implemented to determine the percentage of asbestos-cement and compare it with the percentage obtained using the proposed method, aiming to assess its effectiveness. Additionally, a total of 200 executions of both the correlation method and the proposed method were carried out on a 20x20-pixel section of the image with 380 reflectance bands, in order to calculate the average processing time for each method and evaluate the efficiency of the proposed method relative to the correlation method.

3. Results y Discussion

In terms of the results, the area under the curve of the characteristic pixel of asbestos-cement was first calculated to compare this area with the area under the curve of the sample pixels of asbestos and other materials. Using the implementation of Simpson's method provided by the SciPy library, the area under the curve was calculated to be 63.775, as shown in Figure 4.

Figure 4. Area under the curve of the asbestos spectral signature. Source: Own.

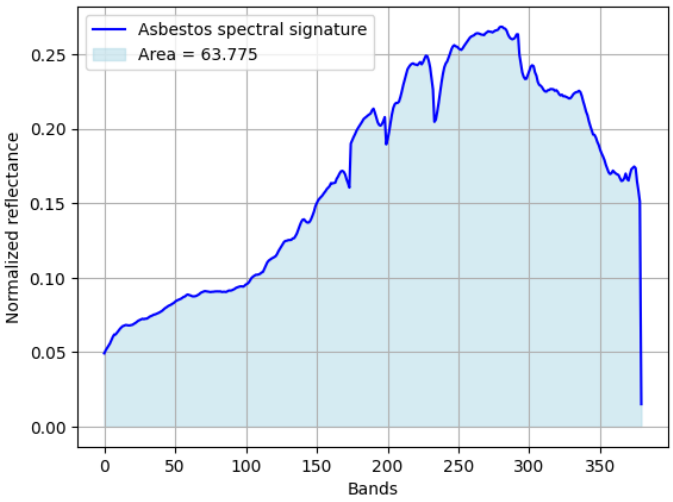

Once the area under the curve of the characteristic pixel was identified for all bands, an iteration was performed for each asbestos-cement pixel and pixels of other materials. For each pixel, the area under the curve and the absolute value of the difference between areas were determined, obtaining the minimum and maximum difference values in each case. Accordingly, Figure 5 presents a graph showing the minimum and maximum difference values obtained for the sample pixels of asbestos and other materials.

Figure 5. Evaluation of the method with asbestos and non-asbestos pixels. Source: Own.

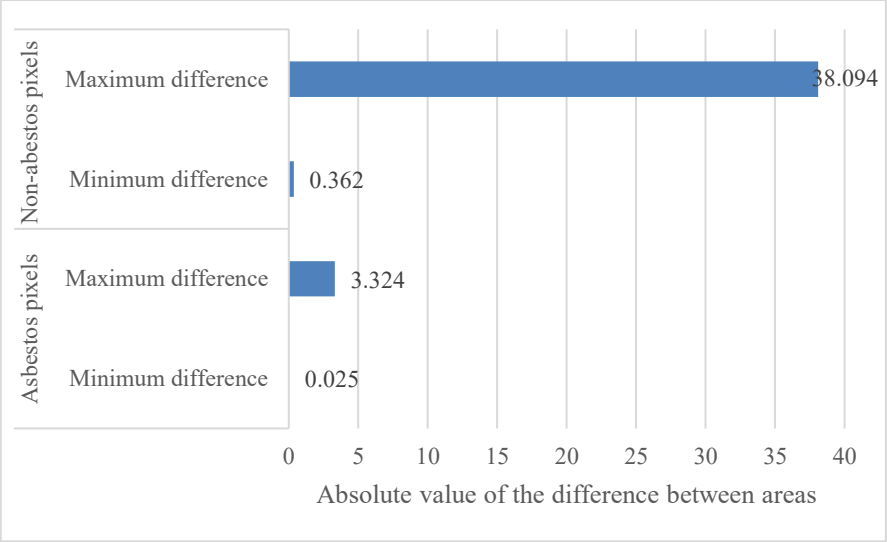

From Figure 5, it can be observed that when considering all 380 bands of the sample pixels of asbestos and other materials, there is an overlap between the absolute maximum difference with asbestos and the absolute minimum difference with non-asbestos pixels. As a result, if all bands are used in the implementation of the method, it will face difficulties in distinguishing some pixels and may confuse asbestos-cement pixels with those of other materials. In this regard, the difference between the maximum threshold with asbestos and the minimum threshold with non-asbestos pixels is -2.962.

Accordingly, the range of bands where the difference between the two aforementioned thresholds was positive was identified, with the results presented in Table 1.

Table 1. Difference between thresholds by band range

Reflectance band range	Difference between thresholds
0-380	-2.962
0-350	-3.168
0-300	-2.674
0-200	-3.109
200-300	-1.077
200-250	-0.052
50-200	-2.322
50-160	0.328
55-160	0.374
55-157	0.491
52-157	0.547
50-157	0.576
48-157	0.602
46-157	0.572

According to the results shown in Table 1, it can be observed that the range with the largest difference between thresholds (the absolute maximum difference with asbestos pixels and the absolute minimum difference with non-asbestos pixels) corresponds to the area between bands 48 and 157, with a difference of 0.602. Figure 6 presents the specific thresholds obtained for this range of bands.

Figure 6. Evaluation of the method with asbestos and non-asbestos pixels in bands 48-157. Source: Own.

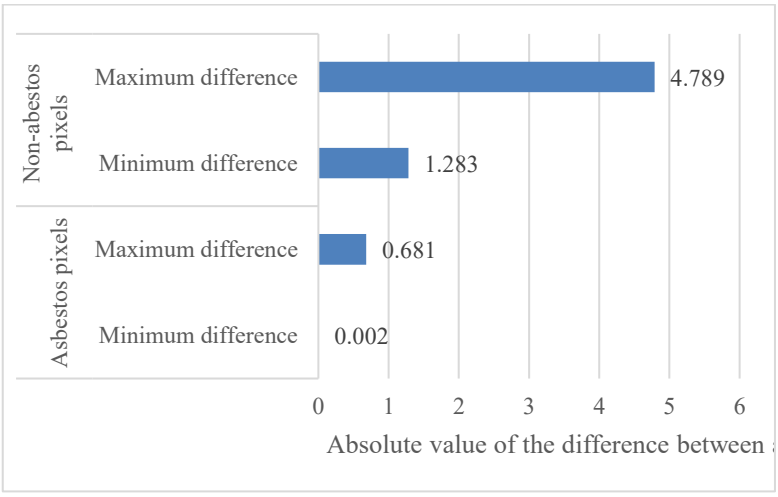

In Figure 6, it can be observed that for the case of bands 48 to 157, the absolute minimum difference with non-asbestos pixels is greater than the absolute maximum difference with asbestos pixels, meaning there is no overlap. This range of bands provides the highest effectiveness of the method in distinguishing asbestos pixels from pixels of other materials. Based on the thresholds identified in Figure 6, the method was then deployed across the entire reference image to determine the percentage of asbestos pixels present. Figure 7 shows both the deployment of the method over the entire image and the asbestos zones detected by the method, marked in blue.

Figure 7. Deployment of the method in the band range 48-157. Source: Own.

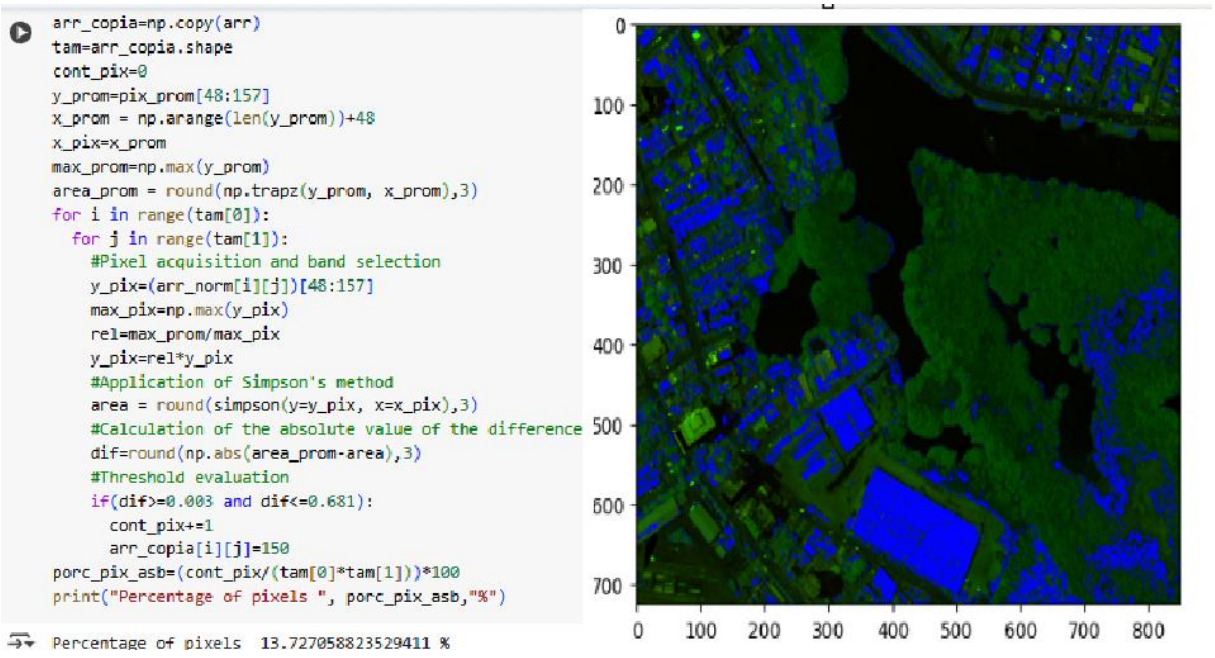

```
arr_copia=np.copy(arr)
tam=arr_copia.shape
cont_pix=0
y_prom=pix_prom[48:157]
x_prom = np.arange(len(y_prom))+48
x_pix=x_prom
max_prom=np.max(y_prom)
area_prom = round(np.trapz(y_prom, x_prom),3)
for i in range(tam[0]):
  for j in range(tam[1]):
    #Pixel acquisition and band selection
    y_pix=(arr_norm[i][j])[48:157]
    max_pix=np.max(y_pix)
    rel=max_prom/max_pix
    y_pix=rel*y_pix
    #Application of Simpson's method
    area = round(simpson(y=y_pix, x=x_pix),3)
    #Calculation of the absolute value of the difference
    dif=round(np.abs(area_prom-area),3)
    #Threshold evaluation
    if(dif>=0.003 and dif<=0.681):
      cont_pix+=1
      arr_copia[i][j]=150
porc_pix_asb=(cont_pix/(tam[0]*tam[1]))*100
print("Percentage of pixels ", porc_pix_asb,"%")
```

```
Percentage of pixels  13.727058823529411 %
```

As a result of applying the method to the band range from 48 to 157, it was found that the method detected 13.73% of asbestos pixels in the entire image. However, visual inspection of Figure 8 reveals that while some areas are correctly detected, certain vegetation pixels are mistakenly identified as asbestos pixels. To compare the effectiveness of the proposed method, the correlation method was applied to the complete image to determine the percentage of asbestos pixels, with the results presented in Figure 8.

Figure 8. Deployment of the correlation method on the reference image.Source: Own.

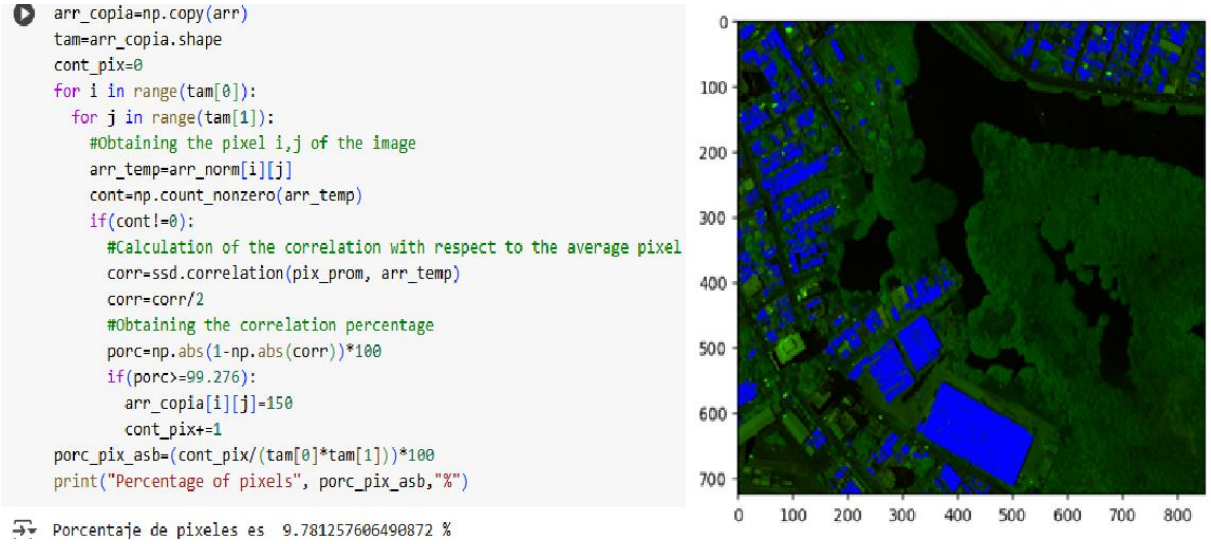

```
arr_copia=np.copy(arr)
tam=arr_copia.shape
cont_pix=0
for i in range(tam[0]):
  for j in range(tam[1]):
    #Obtaining the pixel i,j of the image
    arr_temp=arr_norm[i][j]
    cont=np.count_nonzero(arr_temp)
    if(cont!=0):
      #Calculation of the correlation with respect to the average pixel
      corr=ssd.correlation(pix_prom, arr_temp)
      corr=corr/2
      #Obtaining the correlation percentage
      porc=np.abs(1-np.abs(corr))*100
      if(porc>=99.276):
        arr_copia[i][j]=150
        cont_pix+=1
porc_pix_asb=(cont_pix/(tam[0]*tam[1]))*100
print("Percentage of pixels", porc_pix_asb,"%")
```

```
Porcentaje de pixeles es  9.781257606490872 %
```

From the implementation of the correlation method on the reference hyperspectral image, it was found that the percentage of detected asbestos pixels was 9.78%. This indicates that the proposed method detected 3.95% more pixels than the correlation method, which is not a significant difference. However, it is observed that, unlike the proposed method, the correlation method provides a more accurate detection of asbestos without mistakenly identifying certain vegetation areas as asbestos pixels. To evaluate the computational efficiency of the proposed method compared to the correlation method, 200 executions

of both methods were performed on a 20x20 pixel region of the image with 380 bands, in order to determine the average processing time per execution for each method. Figure 9 presents the average processing times obtained for each method when processing the specified image region.

Figure 9. Evaluation of the average processing time over 200 execution of the correlation method and the proposed method. Source: Own.

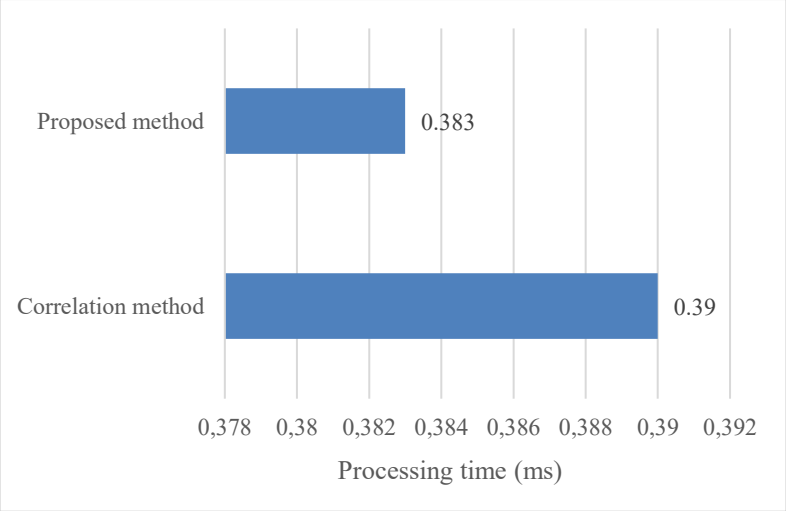

According to the results presented in Figure 9, it can be concluded that the correlation method is 1.02 times slower than the proposed method, meaning that the proposed method is 1.79% more efficient than the correlation method. Thus, the proposed method can be considered a viable alternative to the correlation method, as it achieves a similar level of effectiveness while offering slightly better efficiency. This makes the method suitable for integration into material monitoring systems using hyperspectral images.

As a discussion point, it is important to note that, compared to studies that have not utilized machine learning models for material detection, such as the correlation method [31], this research provides an alternative with comparable results in terms of effectiveness and improved results in terms of efficiency. However, it is crucial to highlight that the proposed method requires a preliminary process to identify the reflectance bands where the area under the curve is effective. As demonstrated in this study, when all 380 bands are used, the method encounters difficulties in distinguishing asbestos-cement pixels from those of other materials.

Similarly, this research demonstrated how the use of open-source tools and technologies enables the implementation and customization of methods for material detection in spectral images. This approach allows for the development of flexible and adaptable solutions tailored to the specific needs of different studies, fostering innovation. This represents a significant contribution compared to remote sensing studies that rely on proprietary tools [39], [40], which face limitations such as difficulty in hybridizing methods and the high cost of licenses barriers that restrict access to these technologies for universities and research centers in developing countries. Furthermore, open-source solutions promote collaboration, transparency, and global accessibility in scientific research. In this way, this research aims to serve as a reference for replication and extrapolation in material detection by educational institutions, research centers, and companies, leveraging the economic and technical advantages of open-source technologies.

The effectiveness and efficiency results obtained become particularly relevant when considered in real world application scenarios. For instance, the method's ability to detect a higher percentage of asbestos in the image 3.95% more than the correlation method enables better delineation of high risk areas in hazard maps. Similarly, the improvement in computational efficiency, though modest (1.79%), can lead to significant reductions in processing time when applied to large images or extensive datasets, which are common in urban or environmental monitoring systems. These features make the proposed method

especially valuable for government institutions, health agencies, and environmental organizations that require fast and accurate responses for informed decision-making.

4. Conclusions and Future Work

Considering the challenge of identifying and evaluating alternative methods for processing and analyzing hyperspectral images, given the large volume of data associated with the different spectral bands of each pixel, this article proposed a new approach for asbestos-cement detection in hyperspectral images using Simpson's method for calculating the area under the curve. Based on the results obtained, it can be concluded that, compared to the correlation method, the proposed method is comparable in terms of effectiveness and slightly more efficient computationally. This method aims to be extrapolated and adapted to various studies focused on the detection of different materials in hyperspectral images. Furthermore, due to its simplicity, the method can be easily integrated and hybridized into material monitoring systems that use hyperspectral images.

When adapting and/or extrapolating this method for the detection of other materials, it is crucial to first identify the range of bands where no overlap is observed between the thresholds obtained from the sample pixels. For this reason, it is important to automate detection using methods and perform iterations across different ranges to more accurately identify the appropriate range. In this study, it was determined that when using all 380 default bands of the image, there was overlap between the absolute maximum difference with asbestos and the absolute minimum difference with other materials. Subsequently, after evaluating different band ranges, it was found that the range with no overlap and the greatest difference between thresholds was between bands 48 and 157. Using this band range, the proposed method detected 13.73% asbestos in the reference image, differing by 3.95% compared to the correlation method. These results suggest that the proposed method can be considered a viable alternative for experimentation with hyperspectral images and its inclusion in material monitoring systems within the field of remote sensing.

To evaluate the computational efficiency of the proposed method compared to the correlation method, 200 executions of both methods were performed on a 20x20 pixel region of the image with 380 bands. The results showed that, on average, the correlation method is 1.02 times slower than the proposed method, meaning the proposed method is, on average, 1.79% more efficient than the correlation method. Although the differences may seem minimal, in the context of analyzing large volumes of images, such as in environmental monitoring with hyperspectral images, this method can be highly useful for obtaining results in less time with an approximation that is close to that of the correlation method. However, as previously mentioned, the efficiency depends on the material being identified, in which case it is necessary to determine the range of bands where the method is most effective.

This study demonstrated the effectiveness of using open-source libraries and technologies for the preprocessing, processing, and analysis of hyperspectral images, showing that they are a viable alternative to conventional proprietary tools commonly used for hyperspectral image analysis. For instance, the spectral library was employed to access reflectance data from the various image bands in the form of NumPy arrays. The SciPy library was used to apply Simpson's method for calculating the area under the curve of the characteristic pixel and other pixels in the image. The NumPy library was utilized for managing spectral band data, calculating the characteristic asbestos pixel, and implementing the correlation method. The pandas library was used to load the coordinates of sample pixels for asbestos and other materials from an Excel file. Additionally, the matplotlib library was employed to generate graphs associated with the spectral signatures of asbestos and other materials. Through this research, the use of these libraries and technologies aims to be promoted in research centers and universities for experimenting with material detection methods in hyperspectral images.

Finally, this work represents a significant contribution to public health by enabling the automated and noninvasive identification of asbestos-cement roofing. This capability is particularly valuable in urban and industrial contexts where asbestos exposure poses a latent risk to the population. The proposed

method can be integrated into territorial monitoring systems aimed at preventing asbestos related respiratory diseases and may serve as a foundation for the development of public policies focused on identification and remediation in contaminated environments.

In summary, the developed method represents not only a novel computational alternative but also a valuable tool for public health. Its ability to detect asbestos accurately, efficiently, and without demanding computational requirements positions it as a practical and scalable solution for real-world environmental and epidemiological monitoring scenarios.

As a future work derived from this research, it is intended to combine Simpson's area under the curve method with the wavelet transform, so that by obtaining the approximate component at different levels, it becomes possible to compare the area under the curve of the characteristic pixel with the area under the curve of the other pixels. Additionally, the method's effectiveness in detecting other materials in environmental contexts will be evaluated, such as identifying vegetation or bodies of water.

Acknowledgments

This article is considered a product in the framework of the project “Formulation of an integral strategy to reduce the impact on public and environmental health due to the presence of asbestos in the territory of the Department of Bolivar,” financed by the General System of Royalties of Colombia (SGR) and identified with the code BPIN 2020000100366. The University of Cartagena, Colombia, and the Asbestos-Free Colombia Foundation executed this project.

References

[1] R. Navalgund, V. Jayaraman, and P. S. Roy, “Remote sensing applications : An overview,” *Curr. Sci.*, vol. 93, pp. 1747–1766, 2007.

[2] J. Awange and J. Kiema, “Fundamentals of Remote Sensing,” 2019, pp. 115–123. doi: 10.1007/978-3-030-03017-9_7.

[3] A. F. Jiménez-López, M. Jiménez-López, and F. R. Jiménez-López, “Multispectral analysis of vegetation for remote sensing applications,” *ITECKNE*, vol. 12, no. 2, Nov. 2015, doi: 10.15332/iteckne.v12i2.1242.

[4] A. K. Torres Galindo, A. F. Gómez Rivera, and A. F. Jiménez López, “Desarrollo de un sistema multiespectral para aplicaciones en agricultura de precisión usando dispositivos embebidos,” *Sist. y Telemática*, vol. 13, no. 33, pp. 27–44, Jun. 2015, doi: 10.18046/syt.v13i33.2079.

[5] A. N. Shiklomanov *et al.*, “Enhancing global change experiments through integration of remote-sensing techniques,” *Front. Ecol. Environ.*, vol. 17, no. 4, pp. 215–224, May 2019, doi: 10.1002/fee.2031.

[6] M. I. Abdulraheem, W. Zhang, S. Li, A. J. Moshayedi, A. A. Farooque, and J. Hu, “Advancement of Remote Sensing for Soil Measurements and Applications: A Comprehensive Review,” *Sustainability*, vol. 15, no. 21, p. 15444, Oct. 2023, doi: 10.3390/su152115444.

[7] J. A. Strong and M. Elliott, “The value of remote sensing techniques in supporting effective extrapolation across multiple marine spatial scales,” *Mar. Pollut. Bull.*, vol. 116, no. 1–2, pp. 405–419, Mar. 2017, doi: 10.1016/j.marpolbul.2017.01.028.

[8] C. Colombero, C. Comina, and A. Godio, “Special Issue ‘Remote Sensing in Applied Geophysics,’” *Remote Sens.*, vol. 12, no. 20, p. 3413, Oct. 2020, doi: 10.3390/rs12203413.

[9] L. Gao and R. T. Smith, “Optical hyperspectral imaging in microscopy and spectroscopy - a review of data acquisition,” *J. Biophotonics*, vol. 8, no. 6, pp. 441–456, Jun. 2015, doi: 10.1002/jbio.201400051.

[10] J. Burger and A. Gowen, “Data handling in hyperspectral image analysis,” *Chemom. Intell. Lab. Syst.*, vol. 108, no. 1, pp. 13–22, Aug. 2011, doi: 10.1016/j.chemolab.2011.04.001.

[11] G. Lu and B. Fei, “Medical hyperspectral imaging: a review,” *J. Biomed. Opt.*, vol. 19, no. 1, p. 010901, Jan. 2014, doi: 10.1117/1.JBO.19.1.010901.

[12] A. A. Gowen, "Near Infrared Hyperspectral Image Analysis Using R. Part 2: Working with Hypercubes," *NIR news*, vol. 25, no. 3, pp. 17–19, May 2014, doi: 10.1255/nirn.1437.

[13] Chein-I Chang, "An information-theoretic approach to spectral variability, similarity, and discrimination for hyperspectral image analysis," *IEEE Trans. Inf. Theory*, vol. 46, no. 5, pp. 1927–1932, 2000, doi: 10.1109/18.857802.

[14] R. M. Willett, M. F. Duarte, M. A. Davenport, and R. G. Baraniuk, "Sparsity and Structure in Hyperspectral Imaging : Sensing, Reconstruction, and Target Detection," *IEEE Signal Process. Mag.*, vol. 31, no. 1, pp. 116–126, Jan. 2014, doi: 10.1109/MSP.2013.2279507.

[15] Abhinav, A. J. S, and S. Singh, "Spectral Signature Analysis of Land Sat TM Images for Improved Hyper Spectral Image Analysis," in *2024 International Conference on Optimization Computing and Wireless Communication (ICOCWC)*, IEEE, Jan. 2024, pp. 1–6. doi: 10.1109/ICOCWC60930.2024.10470851.

[16] G. Bonifazi, G. Capobianco, and S. Serranti, "Asbestos containing materials detection and classification by the use of hyperspectral imaging," *J. Hazard. Mater.*, vol. 344, pp. 981–993, Feb. 2018, doi: 10.1016/j.jhazmat.2017.11.056.

[17] G. Bonifazi, G. Capobianco, and S. Serranti, "Hyperspectral imaging applied to the identification and classification of asbestos fibers," in *2015 IEEE SENSORS*, IEEE, Nov. 2015, pp. 1–4. doi: 10.1109/ICSENS.2015.7370458.

[18] G. Bonifazi, G. Capobianco, and S. Serranti, "Hyperspectral Imaging and Hierarchical PLS-DA Applied to Asbestos Recognition in Construction and Demolition Waste," *Appl. Sci.*, vol. 9, no. 21, p. 4587, Oct. 2019, doi: 10.3390/app9214587.

[19] G. Bonifazi, G. Capobianco, S. Serranti, S. Malinconico, and F. Paglietti, "ASBESTOS DETECTION IN CONSTRUCTION AND DEMOLITION WASTE ADOPTING DIFFERENT CLASSIFICATION APPROACHES BASED ON SHORT WAVE INFRARED HYPERSPECTRAL IMAGING," *Detritus*, no. 20, pp. 90–99, Aug. 2022, doi: 10.31025/2611-4135/2022.15211.

[20] C. Bassani *et al.*, "Deterioration status of asbestos-cement roofing sheets assessed by analyzing hyperspectral data," *Remote Sens. Environ.*, vol. 109, no. 3, pp. 361–378, Aug. 2007, doi: 10.1016/j.rse.2007.01.014.

[21] S. Pascucci, C. Bassani, L. Fusilli, and A. Palombo, "Evaluation of a hyperspectral scanner allowing for deterioration status assessment of asbestos-cement roofing sheets," M. Ehlers and U. Michel, Eds., Oct. 2007, p. 67490V. doi: 10.1117/12.739079.

[22] W. Dong, C. Zhou, F. Wu, J. Wu, G. Shi, and X. Li, "Model-Guided Deep Hyperspectral Image Super-Resolution," *IEEE Trans. Image Process.*, vol. 30, pp. 5754–5768, 2021, doi: 10.1109/TIP.2021.3078058.

[23] W. Yu, M. Zhang, and Y. Shen, "Spatial Revising Variational Autoencoder-Based Feature Extraction Method for Hyperspectral Images," *IEEE Trans. Geosci. Remote Sens.*, vol. 59, no. 2, pp. 1410–1423, Feb. 2021, doi: 10.1109/TGRS.2020.2997835.

[24] D. Datta, P. K. Mallick, A. K. Bhoi, M. F. Ijaz, J. Shafi, and J. Choi, "Hyperspectral Image Classification: Potentials, Challenges, and Future Directions," *Comput. Intell. Neurosci.*, vol. 2022, pp. 1–36, Apr. 2022, doi: 10.1155/2022/3854635.

[25] S. Li, W. Song, L. Fang, Y. Chen, P. Ghamisi, and J. A. Benediktsson, "Deep Learning for Hyperspectral Image Classification: An Overview," *IEEE Trans. Geosci. Remote Sens.*, vol. 57, no. 9, pp. 6690–6709, Sep. 2019, doi: 10.1109/TGRS.2019.2907932.

[26] Z. Zulfiqar *et al.*, "Enhancing Hyperspectral Image Analysis With Deep Learning: An Innovative Hybrid Approach for Improved Detection and Classification Using Deep-Detect," *IEEE Access*, vol. 12, pp. 149272–149287, 2024, doi: 10.1109/ACCESS.2024.3475480.

[27] R. J. Tallarida and R. B. Murray, "Area under a Curve: Trapezoidal and Simpson's Rules," in *Manual of Pharmacologic Calculations*, New York, NY: Springer New York, 1987, pp. 77–81. doi: 10.1007/978-1-4612-4974-0_26.

[28] A. Basu and B. Dutta, "An Analytical Study of Alternative Method for Solving Lotka's Law with Simpson's 1/3 Rule," *J. Scientometr. Res.*, vol. 13, no. 2, pp. 466–474, Aug. 2024, doi: 10.5530/jscires.13.2.37.

[29] Bes Hendi Rio Pardede, Bunga Diviya Kusfa, and Lauren Teresia Tamba, "Penerapan Metode

Trapesium , Metode Simpson 1/3, dan Metode Simpson 3/8 Dalam Integrasi Numerik Menggunakan Software Matlab," *Pentagon J. Mat. dan Ilmu Pengetah. Alam*, vol. 2, no. 4, pp. 24–31, Oct. 2024, doi: 10.62383/pentagon.v2i4.268.

[30] M. Md. Moheuddin, M. Abdus Sattar Titu, and S. Hossain, "A New Analysis of Approximate Solutions for Numerical Integration Problems with Quadrature-based Methods," *Pure Appl. Math. J.*, vol. 9, no. 3, p. 46, 2020, doi: 10.11648/j.pamj.20200903.11.

[31] G. E. Chanchí Golondrino, M. A. Ospina Alarcón, and M. Saba, "Vegetation Identification in Hyperspectral Images Using Distance/Correlation Metrics," *Atmosphere (Basel).*, vol. 14, no. 7, p. 1148, Jul. 2023, doi: 10.3390/atmos14071148.

[32] E. Algranti, E. M. C. Mendonça, E. M. DeCapitani, J. B. P. Freitas, H. C. Silva, and M. A. Bussacos, "Non-malignant asbestos-related diseases in Brazilian asbestos-cement workers," *Am. J. Ind. Med.*, vol. 40, no. 3, pp. 240–254, Sep. 2001, doi: 10.1002/ajim.1095.

[33] N. L. Durán-Ávila, J. R. Cañarte-Murillo, J. N. Zambrano-Murillo, and C. A. Ayón-Lucio, "Daño pulmonar causado por asbestos en trabajadores de la construcción," *CIENCIAMATRIA*, vol. 7, no. 1, pp. 260–270, Aug. 2021, doi: 10.35381/cm.v7i1.529.

[34] R. A. Accinelli and L. M. López, "Asbesto: la epidemia silenciosa," *ACTA MEDICA Peru.*, vol. 33, no. 2, p. 138, Aug. 2016, doi: 10.35663/amp.2016.332.64.

[35] R. C. Gonzalez and R. E. Woods, *Digital Image Processing*. Harlow: Pearson Education, 2018. doi: 10.1201/9781003002826-2.

[36] J. A. Richards, *Remote Sensing Digital Image Analysis*. Cham: Springer International Publishing, 2022. doi: 10.1007/978-3-030-82327-6.

[37] A. Bhargava, A. Sachdeva, K. Sharma, M. H. Alsharif, P. Uthansakul, and M. Uthansakul, "Hyperspectral imaging and its applications: A review," *Heliyon*, vol. 10, no. 12, p. e33208, 2024, doi: 10.1016/j.heliyon.2024.e33208.

[38] Y. E. García-Vera, A. Polochè-Arango, C. A. Mendivelso-Fajardo, and F. J. Gutiérrez-Bernal, "Hyperspectral Image Analysis and Machine Learning Techniques for Crop Disease Detection and Identification: A Review," *Sustainability*, vol. 16, no. 14, p. 6064, Jul. 2024, doi: 10.3390/su16146064.

[39] H. Sabah Jaber and .., "Classification of Hyperspectral Remote Sensing for Production Minerals Mapping Using Geological Map and Geomatics Techniques," *Int. J. Eng. Technol.*, vol. 7, no. 4.20, pp. 480–484, Nov. 2018, doi: 10.14419/ijet.v7i4.20.26247.

[40] S. J. Hussein and Z. Fakhri Merzah, "Analysis of Hyperspectral Remote Sensing Images for Extraction Geological Rock Types Maps by Geospatial Techniques," *IOP Conf. Ser. Mater. Sci. Eng.*, vol. 901, no. 1, p. 012016, Aug. 2020, doi: 10.1088/1757-899X/901/1/012016.